




Genomic mosaicism underlies the adaptation of marine *Synechococcus* ecotypes to distinct oceanic iron niches

Nathan A. Ahlgren ^{1,*} Bernard Shafer Belisle ¹
and Michael D. Lee ^{2,3}

¹Biology Department, Clark University, 950 Main Street, Worcester, MA, 01610, USA.

²NASA Ames Research Center, Exobiology Branch, PO Box 1, Moffett Field, CA, 94035, USA.

³Blue Marble Space Institute of Science, Seattle, WA, 98154, USA.

Summary

Phytoplankton are limited by iron (Fe) in ~40% of the world's oceans including high-nutrient low-chlorophyll (HNLC) regions. While low-Fe adaptation has been well-studied in large eukaryotic diatoms, less is known for small, prokaryotic marine picocyanobacteria. This study reveals key physiological and genomic differences underlying Fe adaptation in marine picocyanobacteria. HNLC ecotype CRD1 strains have greater physiological tolerance to low Fe congruent with their expanded repertoire of Fe transporter, storage and regulatory genes compared to other ecotypes. From metagenomic analysis, genes encoding ferritin, flavodoxin, Fe transporters and siderophore uptake genes were more abundant in low-Fe waters, mirroring paradigms of low-Fe adaptation in diatoms. Distinct Fe-related gene repertoires of HNLC ecotypes CRD1 and CRD2 also highlight how coexisting ecotypes have evolved independent approaches to life in low-Fe habitats. *Synechococcus* and *Prochlorococcus* HNLC ecotypes likewise exhibit independent, genome-wide reductions of predicted Fe-requiring genes. HNLC ecotype CRD1 interestingly was most similar to coastal ecotype I in Fe physiology and Fe-related gene content, suggesting populations from these different biomes experience similar Fe-selective conditions. This work supports an improved perspective that phytoplankton are shaped by more nuanced Fe niches in the oceans than previously implied from

mostly binary comparisons of low- versus high-Fe habitats and populations.

Introduction

Iron (Fe) is an important micronutrient for marine phytoplankton that requires this element for essential processes including photosynthesis and central metabolism. Roughly 40% of the world's oceans are Fe-limited, including the so-called high-nutrient low-chlorophyll (HNLC) regions of the Equatorial and sub-Arctic Pacific and the Southern Ocean (Moore *et al.*, 2002; Moore and Braucher, 2008). These regions represent productive regions that have global significance to marine food webs and carbon cycling, thus it is important to understand how phytoplankton are able to grow and thrive in these regions despite low Fe availability. Seminal work studying low-Fe adaptation in diatoms, large eukaryotic phytoplankton, has revealed key mechanisms by which certain species have adapted to low-Fe conditions (see review in Marchetti and Maldonado (2016)). In brief, these mechanisms involve increased capacities to acquire and store Fe and reduction of their cellular requirements for Fe (Fe quota). Diatoms however only represent one of the major groups of phytoplankton found in HNLC regions, and less is known about low-Fe adaptation in other globally significant groups—particularly smaller phytoplankton such as globally important marine picocyanobacteria.

Prochlorococcus and *Synechococcus*, the two genera comprising picocyanobacteria, are abundant and ubiquitously-distributed marine phytoplankton that together contribute to ~25% of marine net primary production (Flombaum *et al.*, 2013). Both genera are comprised of multiple phylogenetic clades, most of which represent ecotypes—evolutionarily distinct populations adapted to distinct niches (Rocap *et al.*, 2002; Coleman and Chisholm, 2007; Sohm *et al.*, 2015). It has recently been discovered that *Prochlorococcus* and *Synechococcus* each contain two ecotypes (HNLC1 and HNLC2, CRD1 and CRD2, respectively) that are abundant in low-Fe habitats such as the Equatorial Pacific, Benguela upwelling regions, and parts of the Indian Ocean (Rusch *et al.*, 2010; Sohm *et al.*, 2015).

Received 16 August, 2019; revised 4 November, 2019; accepted 30 November, 2019. *For correspondence. E-mail nahlgren@clarku.edu; Tel. (508) 793-7107; Fax. (508)-793-7174.

Comparison of a representative coastal *Synechococcus* strain, WH8020 (ecotype I) to an open-ocean *Synechococcus* isolate WH8102 (ecotype III) has revealed distinct physiological responses to Fe-limitation across two ecotypes; however, similar work that includes HNLC strains is lacking. Recently, several new *Synechococcus* isolates have been cultured and genomes have been sequenced from ecotypes that occupy many diverse oceanic biomes, including from HNLC ecotypes CRD1 and CRD2 (Lee *et al.*, 2019). These provide a valuable resource to better characterize the physiological adaptation and evolutionary genomic signatures underlying low-Fe adaptation in these phytoplankton.

In this study, we characterize the physiological response of ecotype CRD1 strains to low-Fe conditions, provide a comprehensive comparison of Fe-related gene content in *Synechococcus* genomes, and evaluate *in situ* distributions of Fe-related genes in natural populations. Our results reveal how multiple ecotypes have evolved similar, but distinct mechanisms to thrive in low-Fe habitats, often mirroring the same types of adaptations seen in diatoms. Furthermore, comparison across multiple ecotypes abundant in several different marine biomes provides an improved view of how diverse phytoplankton populations have evolved to varied Fe niches in the world's oceans.

Results

Synechococcus ecotype biogeography

We mapped TARA Ocean (Sunagawa *et al.*, 2015) and equatorial Pacific metagenomes (Lee *et al.*, 2019) to reference *Synechococcus* core genes (Table S1) and detected coherent biogeographic patterns of *Synechococcus* ecotypes (Fig. 1A) consistent with previous studies (Zwirgmaier *et al.*, 2008; Sohm *et al.*, 2015; Farrant *et al.*, 2016; Xia *et al.*, 2019). The most abundant ecotypes were partitioned to three major biomes: (i) ecotypes II, III, and X dominate in warm, oligotrophic waters (ii) ecotypes I and IV coexist in cold, higher-nutrient habitats at higher latitudes, including coastal regions, and (iii) ecotypes CRD1 and CRD2 dominate in low-Fe, HNLC regions. (Note that with the availability of CRD2 SAGs we can confirm that clade uncultured ecotype CRD2 first defined by the ITS (Saito *et al.*, 2005) is congruent with clade EnvB independently defined by *petB* (Mazard *et al.*, 2012; Farrant *et al.*, 2016).) Our analysis here further resolves that clades III and X occupy distinct oceanic habitats from ecotype II: clades III and X co-occur and dominate in highly oligotrophic waters (e.g. the Mediterranean Sea) that are particularly low in phosphate (PO_4^{-3}) (Farrant *et al.*, 2016) and in the context of this study, higher in Fe availability (Fig. 1B,

Fig. S1) (Note that PO_4^{-3} and Fe are inversely correlated to one another: $p = 0.02$, Pearson correlation). In particular, locations with clades III and X present have the two highest mean Fe concentrations in comparison to sites where other clades are present (Fig. S1A). The ranges of Fe concentration at which clades II, III and X are found, however, do overlap and their means are not significantly different from each other. Clades III and X nonetheless are the only major *Synechococcus* clades exhibiting significant positive correlations with Fe concentration, and clade II notably does not (Fig. S1B). As such we distinguish ecotype II as 'warm, oligotrophic, midrange-Fe' (II) and ecotypes III and X 'warm, oligotrophic, high-Fe'. Grouping of ecotypes according to these four niches is further supported by non-metric multidimensional scaling (NMDS) analysis and correlations to environmental parameters (Fig. 1B, Fig. S1). In particular, clade III-dominated communities cluster separately from clade-II dominated samples and lie along the axis correlated with Fe concentration in the positive direction with respect to clade II-dominated samples. Also congruent with previous surveys (Farrant *et al.*, 2016; Lee *et al.*, 2019), these seven ecotypes represent the most ubiquitous and prominent *Synechococcus* populations in the global oceans. These ecotypes comprised on average 85% of total recovered *Synechococcus* populations. Here, we have focused on the Fe ecology of these major ecotypes for which metagenomic coverage is sufficient to study ecogenomic trends and for which there were at least two isolate or single cell genomes available to study gene-content differences, with the exception of ecotype X for which only one strain has been sequenced (Table S2). Metagenomic analyses also confirmed fine-scale biogeographic shifts seen in ecotypes II and CRD1 around the Marquesas Islands consistent with patterns of Fe availability there (Caputi *et al.*, 2019) (Fig. 1A, Fig. S2). The waters windward (east) of the islands are dominated by low-Fe adapted ecotype CRD1, while mixing around the islands creates a 'naturally' Fe-fertilized plume of water supporting ecotype II-dominated communities leeward (west) of these islands.

Physiological experiments

Physiological experiments confirmed that ecotype CRD1 strains isolated from HNLC waters were more tolerant of low-Fe conditions than ecotype III strain WH8102. (There are no cultured isolates from clade CRD2). When transferred from Fe replete to low-Fe media, UW179 and GEYO strains grew for longer and at lower Fe levels without signs of Fe-stress—reduced growth rate and differences in size and per cell pigment content—as compared to ecotype III strain WH8102, which rapidly exhibited signs of Fe-stress at 0 and 0.3 nM free

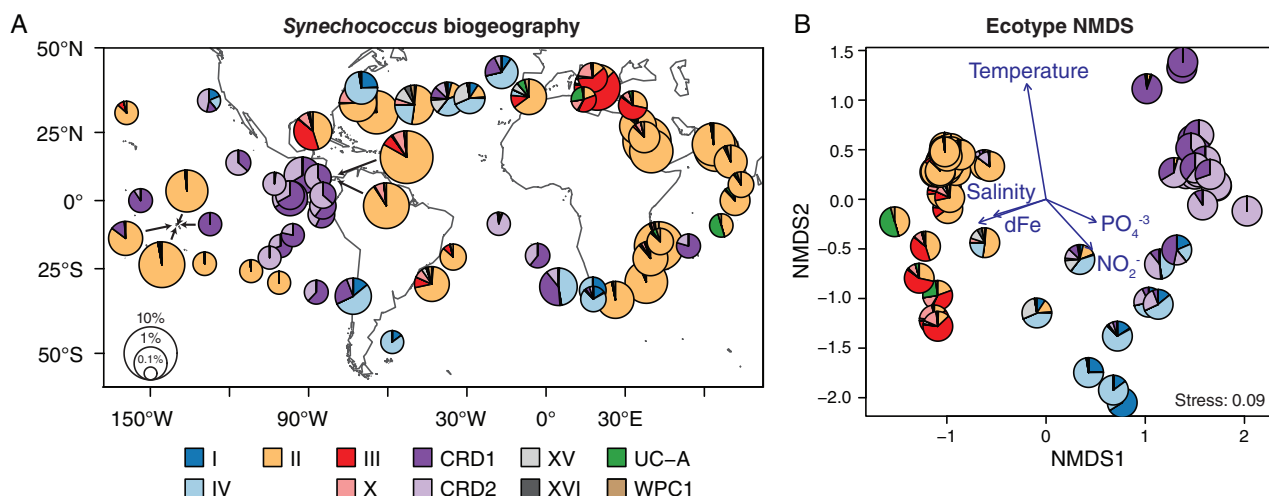


Fig. 1. Biogeography of *Synechococcus* ecotype communities across global ocean surface samples.

A, Map depicting the relative abundance of *Synechococcus* ecotypes for 63 surface samples based on metagenomic read mapping. The radii indicate relative total *Synechococcus* abundance (the fraction of total reads recruiting to *Synechococcus*) and the pie sections depict the relative abundances of *Synechococcus* ecotypes. Clades that did not exceed 2.5% relative abundance in any sample were not plotted (V, VI, VIII, IX and UC-B).

B, Non-metric multidimensional scaling (NMDS) ordination of *Synechococcus* ecotype composition for samples in **A**. Environmental parameters that significantly correlate ($p < 0.05$) to clustering of samples based on *Synechococcus* ecotype community structure are depicted as blue arrows. dFe, dissolved Fe.

inorganic Fe (Fe^{e}) (Fig. 2). Because axenic cultures (free of heterotrophic bacteria) do not yet exist for UW179 and GEYO, the WH8102 culture tested in Fig. 2 was also non-axenic to make reasonable comparisons between strains. Our results for non-axenic WH8102 are consistent with previous experiments done on axenic WH8102 cultures (Mackey *et al.*, 2015), which exhibited signs of Fe stress at ≤ 0.5 nM Fe^{e} . UW179 notably had to be transferred into secondary batch cultures with 0 nM Fe^{e} to observe signs of Fe-limitation. The response of UW179 and GEYO to low Fe conditions more closely resembles that of coastal isolate WH8020 (ecotype I) that showed no evidence of Fe stress even under conditions with 0.004 nM Fe^{e} (Mackey *et al.*, 2015). In addition, the two CRD1 strains were smaller than WH8102 based on normalized forward scatter. Smaller cell size may be advantageous to clade CRD1 cells because of their higher surface area to volume ratio, and diatoms are likewise known to reduce their cell size in response to Fe-limitation (Marchetti and Cassar, 2009).

Genomic analyses

Previous studies have examined the distribution of several Fe-related genes among *Synechococcus* genomes (Palenik *et al.*, 2006; Hopkinson and Morel, 2009; Rivers *et al.*, 2009; Hopkinson and Barbeau, 2012), but without genomes of relevant HNLC ecotypes CRD1 and CRD2. We conducted a comprehensive analysis of Fe-related gene-content across 47 genomes spanning 16 clades

from the three major lineages of marine *Synechococcus* (subclusters 5.1A, 5.1B and 5.3; Fig. 3, Fig. S1). Our analysis included abundant ecotypes from the four major niches to elucidate genomic signatures of Fe niche adaptation (Fig. 3). We initially expected to identify a suite of Fe-related genes that were exclusive to HNLC ecotypes CRD1 or CRD2, but instead we uncovered complex, paraphyletic patterns of gene presence/absence for genes well-characterized to be important in Fe adaptation: Fe acquisition genes, including transporters and siderophore uptake systems; ferritin Fe storage genes; electron transport genes ferredoxin and flavodoxin; and Fe regulatory genes (Fig. 3B). Despite these complex patterns, CRD1 genomes notably had a larger collection of Fe-related genes than other ecotypes. CRD1 genomes have three additional types of Fe^{+2} transporters absent from many other ecotypes: *feoA/B* Fe^{+2} transporter genes; *zupT*, a $\text{Fe}^{+2}/\text{Zn}^{+2}$ transporter from the ZIP family (Zinc-regulated transporters, Fe-regulated transporter-like Proteins) (Eide, 2005); and a Vacuolar Iron Transporter (VIT) family $\text{Fe}^{+2}/\text{Mn}^{+2}$ transporter (Kim *et al.*, 2006) found in two CRD1 strains. The presence of both the *FeoA/FeoB* Fe^{+2} and *IdiA-C* Fe^{+3} ABC transporters in ecotype CRD1, as well as in ecotype I, is striking given that other marine bacteria generally only possess a single dedicated Fe^{+2} or Fe^{+3} transporter (Hopkinson and Barbeau, 2012). The presence of the *FeoA/FeoB* Fe^{+2} transporter is particularly interesting because it was previously thought to be largely absent in marine picocyanobacteria (Hopkinson and Barbeau, 2012).

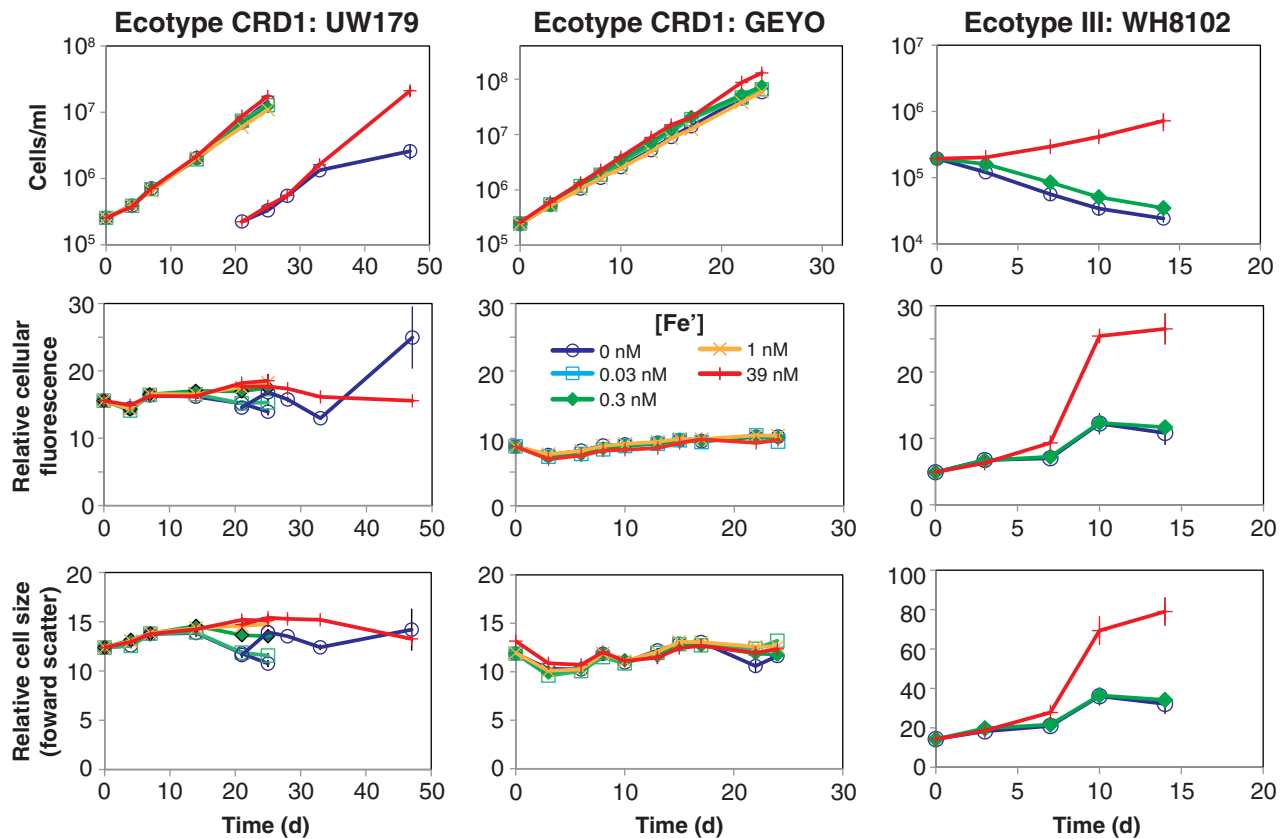


Fig. 2. Response of *Synechococcus* strains to varying Fe availability. HNLC ecotype CRD1 strains UW179 and GEYO and oligotrophic ecotype III strain WH8102 were grown in Sargasso Sea water media with replete Fe (39 nM free inorganic Fe, Fe²⁺) were washed then inoculated in media with various concentrations of Fe. Cells were monitored with a flow cytometer for cell concentration, relative cell size (forward light scatter) and chlorophyll fluorescence per cell (normalized to standard fluorescent beads). Points and bars represent means and standard deviations of triplicate cultures. For UW179, the 0 and 39 nM Fe²⁺ cultures were transferred into fresh media with the same respective Fe levels in order to observe Fe-limitation in the 0 nM Fe²⁺ condition.

Furthermore, the small fraction of uncomplexed Fe in seawater largely exists as Fe⁺³ (Marchetti and Maldonado, 2016), but FeoA/FeoB may be important in a reductive uptake pathway whereby complexed or free Fe⁺³ is reduced and then transported in as Fe⁺² (Shaked *et al.*, 2005; Kranzler *et al.*, 2011; Kranzler *et al.*, 2014). While many ecotypes possess a *zupT* gene, ecotype CRD1, as well as ecotype I, have two copies of this gene. It is important to note that work on ZupT in other bacteria demonstrates that it is a general divalent metal transporter and in *Escherichia coli* it has higher specificity for Zn⁺² than Fe⁺² (Grass *et al.*, 2005; Taudte and Grass, 2010). The specificity of ZupT in cyanobacteria for different divalent metals, however, is unknown. The two CRD2 SAGs interestingly lack the FeoA/B and VIT transporters despite occupying the same habitats as ecotype CRD1, but this could be a consequence of their relatively low estimated completion (Table S2). Ecotype CRD1 curiously lacks a Natural-Resistance-Associated-Macrophage Protein (NRAMP) family divalent metal (including Fe⁺²) transporter (Cellier *et al.*, 2001; Makui *et al.*, 2002)

present in most *Synechococcus* genomes. As with ZupT, the specificity of NRAMP transporters for Fe⁺² or other divalent metals has not been investigated for cyanobacteria.

While previous studies suggested that marine picocyanobacteria largely lack siderophore synthesis or uptake systems (Hopkinson and Barbeau, 2012), this view has recently changed with the discovery of a TonB-dependent siderophore-mediated Fe uptake system in genomes of a *Prochlorococcus* HLII strain, MIT9202 (Hopkinson and Barbeau, 2012), and in *Prochlorococcus* ecotype HNLC2 (a.k.a HLIV) (Malmstrom *et al.*, 2013). Hogle *et al.* (2018a) recently discovered the presence these siderophore uptake genes in marine *Synechococcus*, and we report their presence in full or in part in SAGs from ecotypes CRD2, III, IV and UC-B (Fig. 3B, Fig. S4) (Berube *et al.*, 2018), thereby expanding our view of potential siderophore use in marine cyanobacteria. The lack of these genes in CRD1 genomes also demonstrates how coexisting HNLC CRD1 and CRD2 ecotypes, possess distinct Fe-related gene

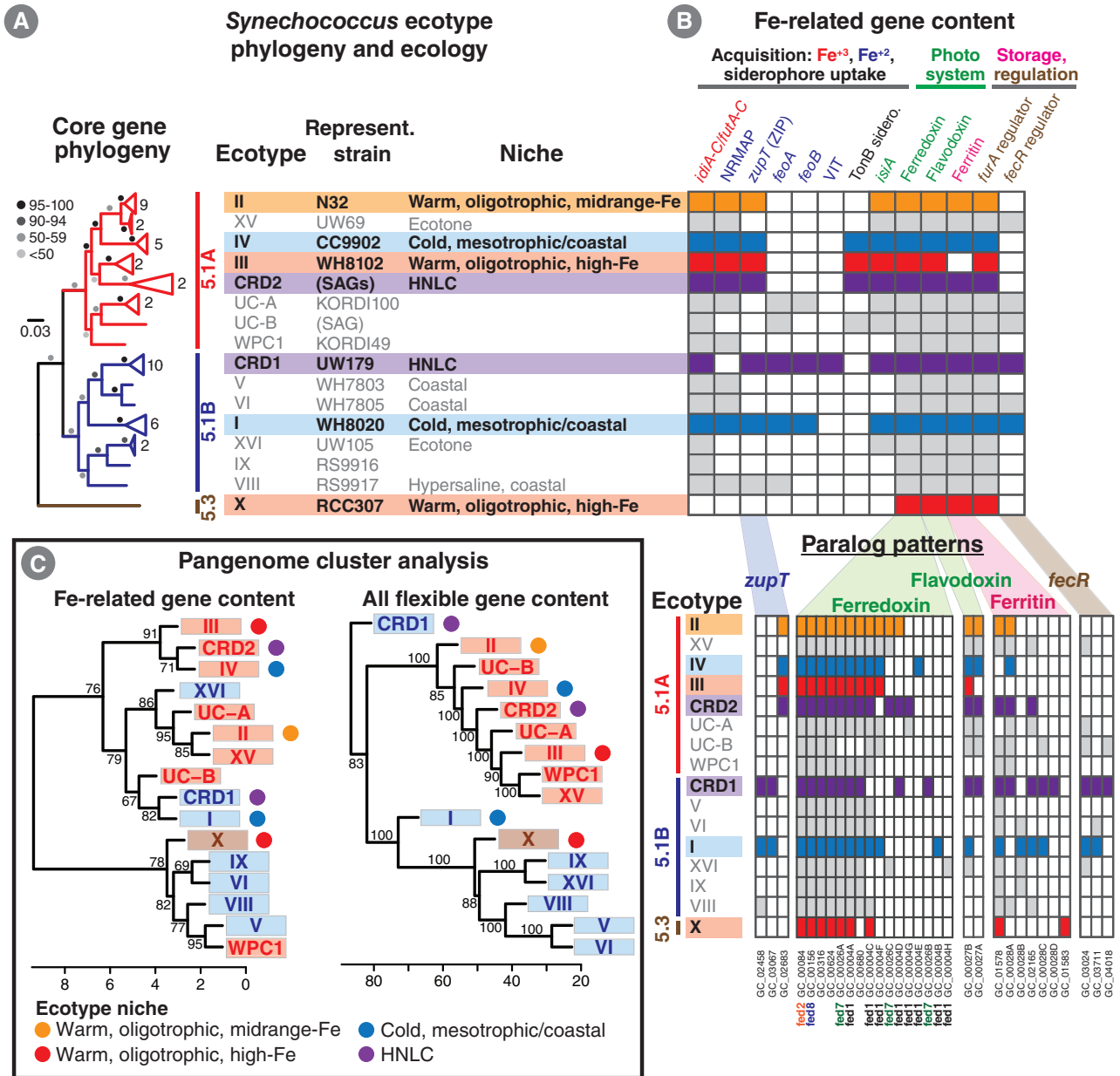


Fig. 3. The distribution of Fe-related genes among *Synechococcus* genomes.

A, The tree and adjacent table summarize the evolutionary history and ecology of *Synechococcus* ecotypes. Core gene phylogeny was based on $n = 139$ single-copy orthologs shared among all incorporated *Synechococcus* reference genomes; dots indicate bootstrap support (see Fig. S3 for full tree). Subclusters 5.1A, 5.1B and 5.3 are indicated by coloured branches and vertical lines (red, blue and brown, respectively). Numbers to the right of triangular tree tips indicate the number of analysed genomes within that clade. The horizontal boxes to the right depict the corresponding ecotype names, a representative strain ('Represent. strain'), and the coherent niche of that ecotype if known. The horizontal boxes, and boxes in the gene presence/absence matrix in B, are coloured according to the four primary niches of the seven most abundant ecotypes in these global ocean samples ($\geq 5\%$ relative abundance in $\geq 10\%$ of samples) (Fig. 1): orange = warm, oligotrophic, midrange-Fe ecotype II; red = warm, oligotrophic, high-Fe ecotypes III and X; blue = cold, mesotrophic/coastal ecotypes (I and IV); and purple = HNLC ecotypes CRD1 and CRD2.

B, The presence and absence of Fe-related genes (columns) among ecotypes, grouped by function: Fe⁺³ (red) and Fe⁺² (blue) transporters and TonB-dependent siderophore uptake operon ('TonB sidero.' black); chlorophyll binding gene *isiA* and photosystem electron transport genes flavodoxin and ferredoxin (green); ferritin iron-storage genes (pink); and Fe-regulation genes *furA* and *fecR* (brown). The presence/absence matrix depicts if at least one genome in each ecotype possesses that gene or operon (filled box), and likewise the patterns of paralogous groups within select gene families are shown below (*zupT*, ferredoxin, flavodoxin, ferritin and *fecR*). Gene cluster names ('GC_XXXXX') are listed below the paralogous gene families (see Table S3). For ferredoxin paralogs, the groups to which they belong ('fedX') are listed below as well, according to classification from freshwater cyanobacteria.

C, Clustering analysis (Wards distance, hierarchical clustering) of ecotypes using the presence/absence of Fe-related genes (left, $n = 52$ clusters) or flexible (non-core) gene content (right, $n = 17,312$ clusters). Fe-related content was analysed using the patterns of individual gene clusters including distinct paralogous gene families. Numbers at the nodes depict bootstrap support (%) for 1000 replicates. Boxes around ecotype names indicate the subcluster to which they belong (5.1A, 5.1B or 5.3) using the colour coding in A, and symbols next to the ecotype names indicate which of the four major niches they occupy (see legend at the bottom).

repertoires. We found no evidence of known siderophore synthesis genes in any picocyanobacterial genomes suggesting that strains with this uptake operon may access Fe bound to siderophores made by other non-picocyanobacterial cells. This could represent an example of the Black Queen hypothesis whereby metabolic functions are shared and distributed among diverse coexisting populations (Morris *et al.*, 2012).

Marine *Synechococcus* possess two different families of known Fe-regulation proteins, FecR (Van Hove *et al.*, 1990) and FurR-like regulators (Shcolnick *et al.*, 2009). CRD1 strains have marginally more copies of *fecR* paralogs than other ecotype strains (mean: 1.5 ± 1.0 vs. 0.26 ± 0.45 , \pm SD; $n = 4, 27$; Welch's *t*-test: $p = 0.09$). This is largely because all three *fecR* paralogs occur in ecotype CRD1, while they are largely absent in most other ecotypes (Fig. S5, Table S3). Ecotype I similarly possesses a second *fecR* paralog (GC_03711) that is notably absent in the other globally abundant *Synechococcus* ecotypes (Fig. 3B, Fig. S5). The FurR protein family in freshwater cyanobacteria includes genes that respond to Fe^{+2} , Zn^{+2} , and peroxide—FurA, Zur, and PerR, respectively—although PerR is also implicated in Fe homeostasis (Shcolnick *et al.*, 2009). Nearly all marine *Synechococcus* contain a single copy of FurA, Zur and PerR, the exceptions primarily being SAGs (Fig. 3B, Table S3).

A striking, emergent pattern is that cold mesotrophic/coastal ecotype I and HNLC ecotype CRD1 possess very similar Fe-related gene content, as supported by clustering analysis (Fig. 3C) revealing a different relationship than seen from core gene phylogeny (Fig. 3A). While this was initially surprising since coastal habitats are typically considered Fe-replete due to terrestrial inputs, coastal waters can experience fluctuating Fe availability and periods of limitation (Hutchins *et al.*, 1995; Hutchins and Bruland, 1998; Bruland *et al.*, 2001; Moore and Braucher, 2008) akin to HNLC habitats. HNLC ecotype CRD2 and coastal ecotype IV likewise are most closely related to one another in terms of Fe-related gene content (Fig. 3C), again distinct from their phylogenetic relationship based on core genes (Fig. 3A).

Patterns of ferredoxin and flavodoxin genes further exemplified the observation of paraphyletic, mosaic-like distribution of Fe-related genes among *Synechococcus* ecotypes (Fig. 3B). Replacement of Fe-containing ferredoxin with Fe-lacking flavodoxin reduces Fe quota, a mechanism by which diatoms achieve adaptation to low-Fe conditions (La Roche *et al.*, 1993; Erdner *et al.*, 1999; Allen *et al.*, 2008). CRD1 isolate genomes possess a higher number of flavodoxin genes on average than other ecotype isolates (2 ± 0 vs. 0.93 ± 0.88 ; ± 1 SD; $n = 4, 27$; Welch's *t*-test: $p < 0.01$), and they differ in the particular paralogs they possess (Fig. 3B, Fig. S6). Patterns

were more complex for ferredoxin, for which we identified 16 paralogous gene families (Fig. 3B, Figs. S7 and S8). CRD1 and non-CRD1 isolates have similar numbers of total ferredoxin genes (9 ± 0 vs. 9.2 ± 1.3 ; \pm SD; $n = 4, 27$; Welch's *t*-test: $p = 0.36$), but CRD1 genomes show distinct patterns in the particular paralogs they possess (Fig. 3B, Table S3). CRD1 strains lack two ferredoxin paralogs present in most other ecotypes (GC_00004C and GC_00004F) but also curiously possess a paralog not found in other ecotypes (GC_00026B; Figs. S7 and S8, Table S3). There were less clear patterns for ferredoxin and flavodoxin genes for ecotype CRD2, in part because there are only two representative SAGs available for this ecotype.

Some diatoms can persist in low-Fe habitats by storing Fe in the protein ferritin during replete conditions that then can be accessed during Fe-limiting conditions (Marchetti *et al.*, 2009; Marchetti *et al.*, 2017). Almost all *Synechococcus* genomes have at least one copy of a ferritin gene, the major exception being the two ecotype III genomes: strain WH8102 and a SAG (Fig. 3B, Table S3). This lack of ferritin in WH8102 is consistent with our physiological experiments (Fig. 2) and the abundance of ecotype III in highly oligotrophic but higher-Fe habitats (Fig. 1A, Fig. S1). CRD1 strains carry more copies of ferritin than other ecotype strains (4.5 ± 1.3 vs. 1.9 ± 1.3 ; \pm SD; $n = 4$ and 27 ; Welch's *t*-test: $p < 0.02$). This is due to ferritin paralogs found uniquely (GC_00028D) or nearly exclusively (GC_00028C) in CRD1 strains and recently duplicated copies within paralog families (Figs. 3B, Fig. S9, Table S3). We also noted that ecotype I on average possesses three ferritin copies, similar to ecotype CRD1, but in contrast, ecotype IV, which cooccurs with ecotype I in the same biome, only carries one ferritin gene (Table S3). This is another example of how ecotypes occupying the same broad niche possess distinct Fe-related gene complements.

We also discovered a clear, genome-wide signature of Fe adaption in marine *Synechococcus*—reduction of predicted Fe-requiring genes in HNLC ecotypes. It was previously observed that metagenome-assembled genomes (MAGs) of *Prochlorococcus* low-Fe ecotypes, HNLC1 and HNLC2 (a.k.a. HLIII and HLIV) lack several Fe-containing proteins found in other *Prochlorococcus* genomes (Rusch *et al.*, 2010). Consistent with this pattern, ecotype CRD1 and CRD2 genomes contain significantly lower proportions of proteins that are predicted to contain Fe-S clusters (Fig. 4). Analysis of a few recently sequenced *Prochlorococcus* HNLC1 and HNLC2 SAGs, and the HNLC MAGs, confirms this same pattern for HNLC ecotypes in comparison to all other high-light (HL) adapted *Prochlorococcus* ecotypes (Fig. 4). Genomes from low-light (LL) adapted *Prochlorococcus* ecotypes have significantly lower proportions of proteins

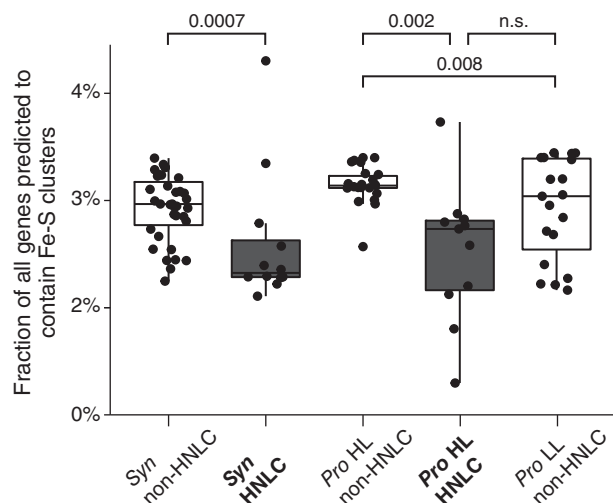


Fig. 4. The fraction of genes predicted as requiring Fe-S clusters by MetalPredator (Valasatava *et al.*, 2016). Results are parsed for genomes from HNLC and non-HNLC clades in *Synechococcus* and *Prochlorococcus*: HNLC *Synechococcus* ecotypes (ecotypes CRD1 and CRD2; 'Syn HNLC'), non-HNLC *Synechococcus* (all other ecotypes, 'Syn non-HNLC'), *Prochlorococcus* non-HNLC high-light (HL) adapted *Prochlorococcus* ecotypes (HL1, HL2; 'Pro non-HNLC'), *Prochlorococcus* HNLC ecotypes (HNLC1, HNLC2; 'Pro HL HNLC'), and non-HNLC low-light (LL) adapted clades (LL1-LLIV; 'Pro LL non-HNLC'). Boxes depict the first and third quartiles, horizontal lines depict the median, and whiskers depict 1.5 times the interquartile range. Statistically significant differences in means between groups are depicted with horizontal brackets with *p*-values listed when is $p < 0.05$ (Pearsons Chi-squared test).

predicted to contain Fe than HL ecotypes, consistent with lower availability of Fe (Sedwick *et al.*, 2005; Fitzsimmons *et al.*, 2015) and evidence of persistent Fe-limitation at deeper portions of the euphotic zone (Sunda and Huntsman, 1997; Hogle *et al.* 2018b). The four HNLC ecotypes from the two distinct genera, *Synechococcus* and *Prochlorococcus*, therefore have undergone similar, convergent changes in their genome evolution. Notably, *Synechococcus* ecotypes CRD1 and CRD2 differ greatly in the particular predicted Fe-S genes that they possess (Fig. S10, Table S4). This, combined with the fact that ecotypes CRD1 and CRD2 arose from two distinct lineages, subclusters 5.1A and 5.1B (Fig. 3A), confirms that these ecotypes have arrived at markedly similar, though distinct adaptations to life in HNLCs via independent, convergent evolution. In contrast, *Prochlorococcus* HNLC ecotypes cluster closest together based on their predicted Fe-S-containing protein complements and are phylogenetically monophyletic, thus the loss of Fe-requiring genes likely occurred before the two ecotypes diverged (Fig. S10).

Examination of losses of predicted Fe-S-requiring revealed one possible example of how HNLC ecotypes may reduce their Fe quotas by replacing Fe-requiring proteins with a homologous protein that does not require Fe. Clades CRD1 and CRD2 genomes conspicuously

lack two Fe-utilizing subunits of glycolate oxidase, *glpC* and *glpE* (GC_01540 and GC_01586), and another subunit *glpD* that does not use Fe. Glycolate is a product of photorespiration whereby ribulose-1,5-bisphosphate carboxylase/oxygenase (Rubisco) reacts with O₂ instead of CO₂ (Eisenhut *et al.*, 2008). Photorespiration results in inefficient carbon fixation via the Calvin cycle, but cyanobacteria can recover this 'lost' carbon by converting glycolate to glyoxylate with glycolate dehydrogenase and subsequent multiple pathways (Eisenhut *et al.*, 2008). We note that clades CRD1 and CRD2 genomes uniquely possess a gene cluster (GC_02882) that based on protein domain homology appears to be a glycolate oxidase (8.41e-153 E-value hit to domain family cd04722: homologous FMN-dependent alpha-hydroxyacid oxidizing enzymes that includes glycolate oxidases; 1.34e-113 E-value hit to domain family PLN02535: glycolate oxidase). Proteins encoded by this gene cluster are not predicted to use an Fe-S cluster and thus likely replaces the activity of Fe-requiring Glp proteins.

Biogeography of Fe-adaptive genes

Surface water metagenomes were used to assess biogeographic patterns and confirm the ecological significance of differences in Fe-related gene content identified above. The coverage of each Fe-related gene-cluster was normalized to *Synechococcus* core-gene coverage ($n = 15$ genes, Table S1) (herein referred to as 'abundances') and were compared between samples binned by Fe level low (<0.3 nM), medium (0.3 to 1 nM) and high (> 1 nM)—using modelled surface water dissolved Fe concentrations (Pasquier and Holzer, 2018). These breakpoints represent relevant thresholds at which marked changes in physiological and protein expression patterns were seen in previous Fe-limitation studies of two marine *Synechococcus* isolates (Mackey *et al.*, 2015). In many cases, gene-cluster abundance patterns were consistent with expected trends and support their ecological importance in Fe adaptation of natural populations. Transporter genes *zupT*, *feoA* and *feoB* genes and total flavodoxin and ferritin gene abundances were significantly more abundant in low-Fe sites (Fig. 5). The abundance of the TonB-dependent siderophore uptake operon was also higher on average in low-Fe waters, although not significantly using this binned approach. Regression analysis however supports that the TonB operon is more abundant at lower Fe availability (Fig. S11). Conversely the NRAMP transporter absent in CRD1 genomes was significantly less abundant in low Fe samples (Figs. S11 and 12). The Fe-S requiring version of glycolate oxidase (*glpC-E*) absent in CRD1 and CRD2 genomes was less abundant in low Fe habitats and conversely the potential alternative, Fe-free glycolate

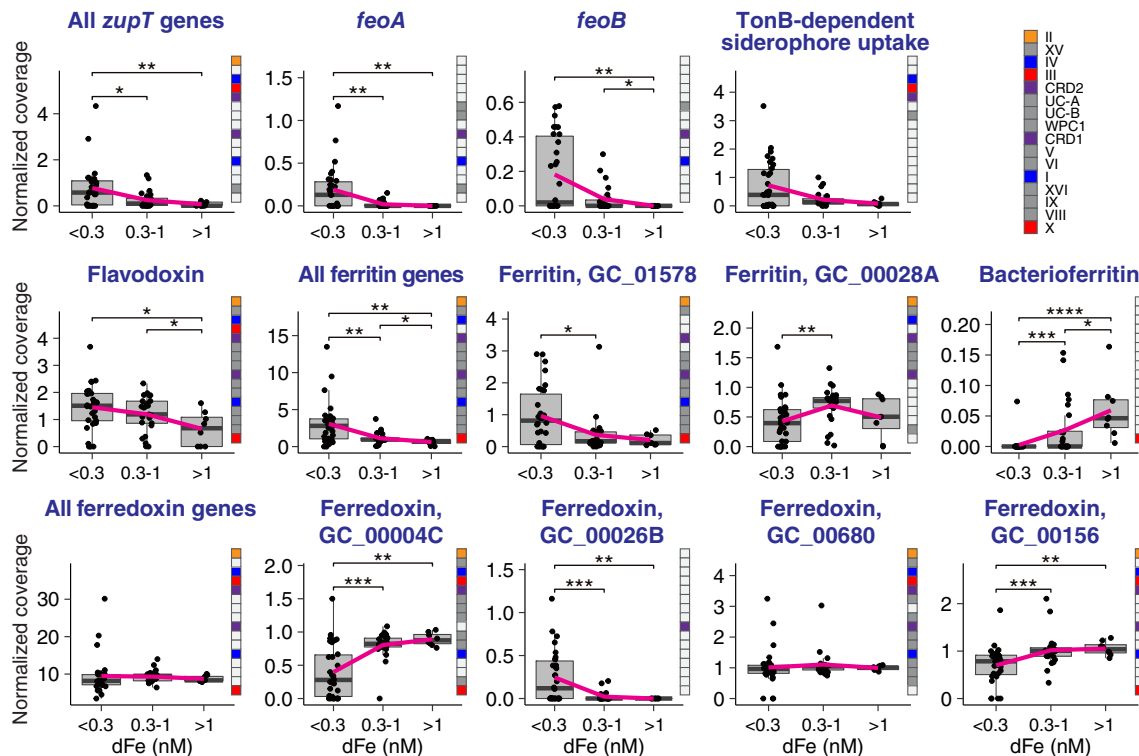


Fig. 5. Normalized abundances of Fe-related genes in global ocean surface samples. Metagenomic gene coverage of gene clusters or operons were normalized to the coverage of 15 core genes found in all *Synechococcus* genomes. Samples were grouped by modelled dissolved Fe concentration, [dFe], (Pasquier and Holzer, 2018) at each site ($n = 34, 18, 11$ for $<0.3, 0.3-1,$ and >1 nM dFe, respectively). 'Siderophore operon' is the TonB-dependent siderophore uptake operon (Fig. S4). Plots with 'All' in the title indicate gene abundance results for all paralogs in that family. For all other plots individual gene cluster results are shown. The column of boxes in each panel indicates the presence/absence of that gene cluster or operon among *Synechococcus* clades (see legend in upper right), as depicted in Fig. 3B. All data points are shown (black dots); horizontal lines within boxplots depict the median; pink lines connect mean values; boxes depict the first and third quartiles; and whiskers depict 1.5 times the interquartile range. Statistically significant differences ($p < 0.05$, Mann-Whitney U test) when present between groups are marked with horizontal brackets and the following notation: '*' = $p < 0.05$, '**' = $p < 0.01$, '***' = $p < 0.001$.

oxidase gene found in CRD1 and CRD2 genomes (GC_02882) was significantly more abundant in low-Fe waters (Figs. S11 and S12), supporting that this is one means by which HNLC strains reduce their Fe quota.

Some gene abundance patterns were more unexpected, including ferredoxin (see below). One example was the Fe-regulation gene, *furA*, which is present in most *Synechococcus* reference genomes, and was detected in somewhat lower levels in low-Fe samples (Fig. S12), although the relationship was not significant using regression analysis (Fig. S11). Another example was bacterioferritin, a distinct family of ferritin present only in ecotype X strain RCC307 (Fig. 3, GC_15834). In contrast to most other ferritin paralog clusters, this gene was more abundant in higher Fe habitats (Figs. S11 and S12), consistent with ecotype X being generally found in higher Fe habitats (Fig. 1, Fig. S1). The protein IsiA binds chlorophyll and is induced under Fe stress. It was previously noted that some oceanic *Synechococcus* strains lack *isiA* (Rivers *et al.*, 2009; Scanlan *et al.*, 2009), but our updated analysis shows that most strains possess *isiA*

(Fig. 3). *isiA* in natural *Synechococcus* populations was recently found to be more abundant in Fe-limited waters, as determined by the ratio of $[\text{NO}_3^-]:[\text{Fe}]$ (Li *et al.*, 2019). In agreement, we found that *isiA* gene abundance was significantly lower in lower-Fe waters by regression analysis (Fig. S11) and by binned Fe level (Fig. S12) but not by $[\text{NO}_3^-]:[\text{Fe}]$. Since the Li *et al.* paper used a qPCR approach to measure *isiA* abundance, primer bias may be behind why we see conflicting results for correlation of $[\text{NO}_3^-]:[\text{Fe}]$ with *isiA*. The VIT family $\text{Fe}^{+2}/\text{Mn}^{+2}$ transporter found exclusively in some CRD1 genomes was only detected in a few surface water samples (Fig. S12).

In contrast to the clear signal of high flavodoxin gene abundance in low Fe samples, total ferredoxin abundance however did not vary significantly across the three Fe levels. The patterns of particular ferredoxin paralogs however were varied and often consistent with their presence or absence in HNLC ecotypes. The paralogs largely absent in CRD1 genomes (GC_00004C, GC_00004F) were less abundant in low Fe habitats and vice versa for paralogs found only in ecotype CRD1 (GC_00026B) or

only in ecotypes CRD2 and UC-A (GC_00004G) (Fig. 5, Figs. S11 and S12). For seven other ferredoxin paralog families found in nearly all *Synechococcus* (GC_00084, GC_00316, GC_00156, GC_00624, GC_00680, GC_00026A and GC_00004A), four showed no significant differences across the three Fe levels, but three were significantly less abundant in lower Fe samples (GC_00156, GC_00624, GC_00680; Fig. 5, Figs. S11 and S12), consistent with the model that low-Fe conditions select for the loss of ferredoxin.

We also note a few other interesting examples where Fe-related genes exhibited paralog- or ecotype-specific patterns. Aside from the broader pattern that total ferritin gene abundance was higher in low-Fe waters (Fig. 5), two paralogs were more abundant in 0.3–1 or > 1 nM Fe samples: bacterioferritin in ecotype X genomes (described above) and paralog GC_00028A found in several ecotypes (Fig. 5, Figs. S11 and S12). Likewise, the abundance pattern of the three *fecR* paralogs differed from each other, suggesting they may have different ecological functions (Fig. S12). The TonB-dependent siderophore uptake operon genes from ecotypes CRD2 were more abundant in low-Fe waters, while conversely ecotype III siderophore uptake genes were more abundant in 0.3–1 and/or > 1 nM Fe samples (Figs. S11 and S12). Similarly, an extra copy of *idiA/futA* present in ecotype III and X genomes (GC_03030) was found to be more abundant in high Fe waters, consistent with the prevalence of both of these ecotypes in higher Fe waters.

Discussion

Analysis of Fe-related gene content across *Synechococcus* ecotypes reveals an overwhelming pattern of complex, pangenome mosaicism, a theme previously seen for marine picocyanobacteria (Kettler *et al.*, 2007; Dufresne *et al.*, 2008). This pattern is best exemplified by ferredoxin and flavodoxin, which in sum are found in all genomes but exhibit notable differences between HNLC and non-HNLC ecotypes when looking at particular paralog families. These different paralogs likely play distinct physiological roles, such that the differential combination of these genes helps confer adaptation to different regimes of Fe availability. Indeed, it is known that different ferredoxin paralogs in the freshwater cyanobacterium *Synechocystis* PCC6803 have distinct physiological roles; are expressed differently under distinct stress conditions; and are in some cases dispensable (Cassier-Chauvat and Chauvat, 2014). Mackey *et al.* likewise observed that ferredoxin paralogs in both coastal and open-ocean strains were expressed either constitutively or only under high Fe conditions, suggesting they have different roles in Fe homeostasis and stress (Mackey *et al.*, 2015). These paralogs belong to gene clusters

GC_00026A and GC_00316, which are found in nearly all *Synechococcus* reference genomes and do not exhibit significant differences across natural samples binned by Fe level. This highlights the importance of conducting expression studies to further elucidate their physiological roles (see below).

We suggest that ferritin paralogs likewise have distinct functions such as managing intracellular, extracellular and/or diel fluctuations in Fe levels (Botebol *et al.*, 2015). For example, ferritin paralog GC_00028B in coastal strain CC9311 was recently suggested to play a novel role in metal detoxification based on structural and biochemical analysis (Bradley *et al.*, 2019). Consistent with this, the paralog was most abundant at sites with intermediate levels of Fe (0.3–1 nM) that also likely have higher concentrations of other toxic metals. Differences in the abundance of the various ferritin paralogs suggest they have different ecological functions and further work is needed to characterize these different forms.

Differential regulation of functionally distinct paralogs can allow for more complex and physiological responses to varied Fe conditions. This model is partially validated with observations that coastal strain WH8020 (ecotype I) has a more complex and tiered regulation of Fe-related genes than the open-ocean isolate WH8102 (ecotype III) (Mackey *et al.*, 2015). This makes sense given that ecotype I likely experiences more fluctuations in Fe availability, including periods of Fe-limitation, than ecotype III does (Mackey *et al.*, 2015). Furthermore, Mackey *et al.* found that the two *FurA* paralogs (isoforms) in strain WH8020 had distinct expression patterns in low (<0.3 nM) versus mid-range (0.3–1 nM) Fe, likely helping to drive the tiered regulation of Fe-adaptive genes. Indeed, we find that distinct paralogs of Fe regulation genes *furA* and *fecR* show different abundance patterns in natural populations and likely are important in creating distinct regulatory networks among ecotypes occupying distinct Fe niches. While our gene abundance results generally confirm the predicted ecological significance of Fe-related genes in the oceans, expression studies and ultimately further molecular characterization are critical for further understanding their roles in Fe-stress responses. In particular, we predict that HNLC ecotypes will have more complex, tiered, Fe-responsive regulation patterns, more similar to those of coastal ecotypes like strain WH8020 than to oligotrophic, high-Fe ecotype III strain WH8102.

Analysis of Fe-related gene content and biogeography highlight how multiple *Synechococcus* have evolved in parallel to occupy similar niches in terms of Fe availability. Ecotypes CRD1 and CRD2, and ecotypes I and IV, clearly have each evolved independently to co-occupy HNLC and cold, mesotrophic habitats (including coastal waters), respectively. In addition, the cross-biome

ecotype pairs, I with CRD1 and IV with CRD2, are intriguingly more closely related to each other in terms of Fe-gene complements than by core-gene phylogeny. This observation suggests that the two distinct biomes they occupy, HNLC and coastal habitats, in fact share similar Fe conditions, namely fluctuating Fe-availability and often Fe-limiting conditions that have selected for similar Fe-related gene repertoires. This conclusion is also supported by initial physiological evidence that ecotype I and CRD1 strains both exhibit higher tolerances for low-Fe conditions ((Mackey *et al.*, 2015) and Fig. 2). It is important to note that the physiological experiments in this study were done on non-axenic cultures, and the heterotrophic bacteria could potentially impact observed physiological responses to Fe availability. However in the case of WH8102, our results with a non-axenic culture are consistent with previous experiments done on axenic WH8102, indicating negligible impact on Fe physiology. Heterotrophic bacteria could potentially enhance Fe uptake in the CRD1 strains, for example, via siderophores; however, CRD1 strains UW179 and GEYO do not encode any apparent siderophore uptake genes. Heterotrophic bacteria could also potentially enhance Fe availability through remineralization from dead cells or refractory forms of Fe, and on the other hand, they also likely compete with *Synechococcus* for Fe. Efforts are on-going to render the CRD1 strains axenic, but the available results with non-axenic cultures are consistent with biogeographic evidence that CRD1 are more tolerant of low-Fe conditions.

This apparent genomic and physiological similarity between HNLC and coastal ecotypes is perhaps not surprising since coastal and HNLC habitats both experience Fe-limitation (Hutchins *et al.*, 1995; Hutchins and Bruland, 1998; Bruland *et al.*, 2001; Moore and Braucher, 2008; Hogle *et al.* 2018b) and they share overlapping niche space in terms of macronutrient and chlorophyll concentrations (Fig. S1). An important distinction between the coastal and HNLC regions may be how persistent and intense Fe-limitation is between them. More time-series studies are needed in both regions to make quantitative comparisons between them, but HNLCs probably experience more chronic and intense (i.e. lower levels of available Fe) limitation than coastal regions. While HNLC genomes and samples analysed here are mostly from low-latitude, warm HNLC habitats, there are cold, high-latitude HNLCs (e.g. the North Pacific, North Atlantic and Southern Ocean) and CRD1 (but not CRD2) in fact sometimes cooccurs with ecotypes I and IV in North Atlantic and North Pacific waters (Fig. 1, (Sohm *et al.*, 2015; Lee *et al.*, 2019; Xia *et al.*, 2019)). Ecotype CRD1 furthermore contains subpopulations that are preferentially found in low- or high-latitude HNLCs as detected by marker gene methods (Farrant *et al.*, 2016;

Xia *et al.*, 2019). Sampling of high-latitude HNLCs however was not extensive enough in the metagenomic data sets used here to resolve such CRD1 subclade differences. Additional metagenomic surveys and isolates of high-latitude HNLC strains will be valuable to investigate such within-ecotype subpopulations.

Sohm *et al.* first highlighted this pattern of prevalent convergent evolution of *Synechococcus* and *Prochlorococcus* ecotypes whereby distinct lineages have come to occupy the same niches. Our analysis here highlights how the modes of ecotype evolution between these two genera appear to fundamentally differ. *Synechococcus* is characterized by frequent parallel evolution of multiple ecotypes sharing similar niches, while *Prochlorococcus* displays more sequential, hierarchical emergence of major ecotypes (Coleman and Chisholm, 2007; Martiny *et al.* 2009a). This is best exemplified by the parallel evolution of *Synechococcus* HNLC ecotypes CRD1 and CRD2 from distinct subcluster lineages in *Synechococcus*, while *Prochlorococcus* HNLC ecotypes HNLC1 and HNLC2 (a.k.a. HLIII and HLIV) appear to have evolved from a recent, common ancestor (Fig. 3, Fig. S10).

This pattern of mosaic pangenome distribution mediated by HGT is a hallmark of prokaryotic populations, in this case contributing to *Synechococcus*' ability to occupy diverse oceanic habitats. The paraphyletic distribution of Fe-related genes in *Synechococcus* is similar to the distribution of adaptive genes to N and P in marine picocyanobacteria, which often show stronger correspondence to the niches they occupy and population biogeography rather than purely to core genome phylogenetic relationships (Martiny *et al.*, 2006; Martiny *et al.* 2009b; Biller *et al.*, 2015; Kashtan *et al.*, 2017; Berube *et al.*, 2019). Here we highlight how Fe-related genes can be combined in different ways to arrive at distinct approaches to living in similar niches, and genomic mosaicism is an important theme more broadly in metal acquisition and tolerance in marine bacteria (Stuart *et al.*, 2009; Stuart *et al.*, 2013; Hogle *et al.*, 2016). On-going work must take into consideration that currently-defined ecotypes appear to contain multiple ecologically distinct populations (Kashtan *et al.*, 2014; Farrant *et al.*, 2016; Kent *et al.*, 2016; Ahlgren *et al.*, 2019), with significant physiological and genomic variation (Kashtan *et al.*, 2014; Pittera *et al.*, 2014). In particular, it will be interesting to examine genomic and physiological diversity among CRD1 subpopulations as more genomes and isolates become available.

Marine *Synechococcus* appear to possess similar general mechanisms of low-Fe adaptation in comparison to marine diatoms—reduction in Fe quota and increased capacity for Fe uptake and storage. Thus, we observe convergent evolution across these very divergent groups

of eukaryotic and prokaryotic phytoplankton. In some cases, both groups use homologous genes and mechanisms to achieve these adaptations: ferritin and altering the balance of ferredoxin and flavodoxin. At the same time, *Synechococcus* uses different genes and mechanisms: the prokaryotic transporter genes *feoA/feoB*, bacterioferritin and siderophore uptake genes that are generally absent in diatoms (Kazamia *et al.*, 2018). An abundance of *Synechococcus* genomes paired with detailed knowledge of ecotype biogeography has allowed for powerful comparisons across these closely-related phytoplankton populations in ways not currently feasible for diatom species. This is largely because diatoms have much bigger, and more complicated, genomes, and as such only a handful have been sequenced and assembled. This makes it difficult to make more global comparisons of modes of genomic evolution between these prokaryotic and eukaryote phytoplankton. However, given that bacteria generally experience higher rates of horizontal gene transfer than eukaryotes (Ochman *et al.*, 2000; Ku and Martin, 2016), we posit that a distinct feature of Fe adaptation in cyanobacteria is extreme flexibility in Fe-adaptive gene content.

Much of our previous understanding of low-Fe adaptation in phytoplankton is often framed by binary comparisons of high-Fe, coastal versus low-Fe, open-ocean habitats, or HNLC versus non-HNLC regions and isolates. This study instead demonstrates how there are multiple and more nuanced Fe niches to which marine phytoplankton are adapted. We have delineated distinct midrange- or high-Fe oligotrophic populations and found that the seemingly disparate biomes of primarily warm HNLCs and cold, mesotrophic waters appear to experience similar selective Fe-selective conditions. Given that *Synechococcus* are easy to isolate in culture and are found in nearly every marine habitat (Flombaum *et al.*, 2013), they provide an excellent model for on-going studies of how phytoplankton populations are adapted to the full variety of Fe regimes in the oceans. We predict that similar, complex Fe niche-differentiation occurs in other phytoplankton groups, like diatoms, but has yet to be uncovered. Moving forward, assessment and modelling of Fe constraints on phytoplankton production should take into consideration this more robust perspective on the diverse Fe niches that occur in the oceans.

Materials and methods

Fe physiology experiments

All cultures (WH8102, MITS9220 and GEYO) used were not axenic and contained heterotrophic bacteria from normal propagation in the lab—that is, heterotrophic bacteria were not transplanted from one culture to another.

Preparation and growth of cultures was done following strict trace-metal clean protocols (use of acid-washed bottles and tubes; Chelex-treated macronutrients; and a trace-metal clean, HEPA-filtered, laminar hood). Cultures were grown at 23 °C under 20 $\mu\text{mol Q m}^{-2} \text{ s}^{-1}$ light (cool white fluorescence lamps) with a 14:10 light dark cycle. Replete Fe media consisted of Sargasso Sea water amended with Pro99 nutrient levels (Moore *et al.*, 2007) with 100 μM EDTA added and the $[\text{FeCl}_3]$ was changed to 1 μM corresponding to an inorganic free Fe (Fe') concentration of 39 nM following the calculations and empirical validation of (Mackey *et al.*, 2015). The total dissolved $[\text{Fe}]$ in the Sargasso sea water (aged >1 yr in an acid washed carboy) used as the media base was 0.03 nM (measured using a seawater preconcentration system [seaFAST] with offline sector-field inductively coupled plasma mass spectrometry [SF-ICP-MS] (Jackson *et al.*, 2018; Wuttig *et al.*, 2019)) and thus contributed negligibly ($\sim 1 \text{ pM}$) to background $[\text{Fe}']$. Cultures were pelleted and washed twice in sterile Sargasso Sea water and then transferred into media where Fe' was changed to 0 (no added Fe, ~ 0.001), 0.03, 0.3, 1, or 39 nM Fe' . Cultures were monitored on a Becton Dickinson Accuri C6 flow cytometer to measure cell concentration, relative cellular chlorophyll fluorescence (excitation: 488 nm, emission: >670 nm long pass filter) and relative cell size (forward light scatter). Fluorescent beads were added to samples to normalize the latter two parameters measured between sampling dates.

Sequence data curation, preparation and analysis

Genomes of marine *Synechococcus* cultured isolates and single-cell amplified genomes (SAGs) with >60% estimated genome completeness (Berube *et al.*, 2018) were downloaded from NCBI and were 'dereplicated' with dRep v2.2.2 (Olm *et al.*, 2017) with default settings other than '-comp 60 -nc 0.5 -sa 0.98' resulting in 47 genomes spanning 16 ecotypes used in subsequent analyses (Table S2). *Prochlorococcus* genomes analysed included the 52 isolate genomes from (Biller *et al.*, 2014) and two metagenome-assembled genomes (MAGs) HNLC1 and HNLC2 (Malmstrom *et al.*, 2013) (Table S5). Orthologous clusters of genes (designated as 'GC_XXXXX') were determined using OrthoMCL (Li *et al.*, 2003) within the anvio platform v5.2 (Eren *et al.*, 2015). Functional annotations available from NCBI's Prokaryotic Genome Annotation Pipeline (PGAP) (Tatusova *et al.*, 2016) were also downloaded, and these were supplemented with additional annotations ascribed via HMM searches (HMMER3; v3.2.1) (Eddy, 2011) of predicted proteins against the Pfam database (release 32) (El-Gebali *et al.*, 2019) and blastp searches against the COG database (Galperin *et al.*, 2015). These were also done within anvio, using

default settings other than specifying blastp for the COG search. Genes involved in Fe physiology were screened by searching gene annotations and conserved domain (CDS) search results (i.e., to Pfam, COG databases) with relevant terms (e.g. 'Fe', 'iron', 'siderophore', 'ferredoxin', 'ferritin', 'flavodoxin') and then inspected manually, including blastp similarity analysis against well-characterized Fe-related genes from freshwater and marine cyanobacteria. Paralogous Fe-related gene clusters (those with more than one gene copy per genome) were further resolved into distinct paralog families using amino acid phylogenies constructed using PhyML (Guindon *et al.*, 2010).

Metagenomic read recruitment to surface, microbial TARA Oceans metagenomes (Sunagawa *et al.*, 2015) and Costa Rica Dome metagenomes (Lee *et al.*, 2019) (Table S6) was performed using bowtie2 v2.3.4 (Langmead and Salzberg, 2012) with default settings and requiring that at least 50% of the reference base pairs recruit reads for that data (genome or gene recruitment) to be included in subsequent analyses. Recruitment to 15 orthologous, single-copy core genes found in all incorporated *Synechococcus* genomes was used to determine ecotype relative abundances (Table S1, Fig. S3). Core gene recruitment results correlated strongly to results using recruitment to whole genomes (Fig. S13). Proteins predicted to require Fe were identified with MetalPredator using the default settings (Valasatava *et al.*, 2016). MetalPredator searches query proteins against libraries of Hidden Markov Model profiles for proteins with Pfam domains or structural motifs that bind Fe-S clusters, and the method predicted Fe-S-binding proteins as those with resulting e-values that are below calibrated e-value thresholds that minimize false-positive results. We reasonably assumed that the particular regions of the genome recovered in SAGs were random so calculation of the fraction of genes predicted to require Fe was the same for SAGs and complete or nearly complete isolate genomes: the number of genes predicted to contain Fe-S clusters divided by the total number of genes in the genome. Processing code for accessing and dereplicating genomes, mapping the TARA dataset, and running the pangenomic workflow is available at the following repository: <https://figshare.com/projects/Ahlgren-Belisle-Lee-EM-2019/73416>.

Statistical analyses

Analyses were performed with the open-source statistical computing language and environment R (Team, 2018). Hierarchical clustering of ecotypes by the gene presence/absence matrices was done using Ward distance, and confidence in these cluster results was assessed using bootstrap analysis with 1000 replicates. The presence of

Fe-related genes or all non-core genes was summarized for each ecotype by assessing if at least one genome in each ecotype possessed that gene.

Environmental data for TARA Oceans samples was obtained from PANGAEA (Tara Oceans Consortium, 2015) (temperature, salinity, phosphate, nitrate+nitrite, nitrite, chlorophyll *a*). Modelled dissolved Fe (dFe) data were taken from (Pasquier and Holzer, 2018) or from (Toulza *et al.*, 2012) for Red Sea sites not predicted by Pasquier and Holzer (2018) (Fig. S14). NMDS analysis was performed using the R package *vegan* (Oksanen *et al.*, 2011) using Bray-Curtis distances. Significant correlation of environmental parameters to ordination by *Synechococcus* ecotype composition was evaluated using the function 'envfit' in *vegan*. Mann-Whitney U tests were used to test statistically significant differences between binned samples for Fe-related gene recruitment values, which were normalized to *Synechococcus* core gene recruitment, and Pearson correlations were tested for gene abundances versus the log of dFe.

Acknowledgements

NAA and BSB performed the physiology experiments. NAA and ML performed the genomic and metagenomic analyses and NAA wrote the paper. We thank N. Cohen and M. Saito for seawater Fe measurements. We thank A. Thompson for helpful feedback on the manuscript and M. Ahlgren for editing of the figures.

References

- Ahlgren, N.A., Perelman, J.N., Yeh, Y., and Fuhrman, J.A. (2019) Multi-year dynamics of fine-scale marine cyanobacterial populations are more strongly explained by phage interactions than abiotic, bottom-up factors. *Environ Microbiol* **21**: 2948–2963. <https://doi.org/10.1111/1462-2920.14687>.
- Allen, A.E., Laroche, J., Maheswari, U., Lommer, M., Schauer, N., Lopez, P.J., *et al.* (2008) Whole-cell response of the pennate diatom *Phaeodactylum tricorutum* to iron starvation. *Proc Natl Acad Sci U S A* **105**: 10438–10443.
- Berube, P.M., Biller, S.J., Hackl, T., Hogle, S.L., Satinsky, B. M., Becker, J.W., *et al.* (2018) Single cell genomes of *Prochlorococcus*, *Synechococcus*, and sympatric microbes from diverse marine environments. *Scientific data* **5**: 180154.
- Berube, P.M., Rasmussen, A., Braakman, R., Stepanauskas, R., and Chisholm, S.W. (2019) Emergence of trait variability through the lens of nitrogen assimilation in *Prochlorococcus*. *Elife* **8**: e41043.
- Biller, S.J., Berube, P.M., Berta-Thompson, J.W., Kelly, L., Roggensack, S.E., Awad, L., *et al.* (2014) Genomes of diverse isolates of the marine cyanobacterium *Prochlorococcus*. *Scientific data* **1**: 140034.

- Biller, S.J., Berube, P.M., Lindell, D., and Chisholm, S.W. (2015) *Prochlorococcus*: the structure and function of collective diversity. *Nat Rev Microbiol* **13**: 13–27.
- Botebol, H., Lesuisse, E., Sutak, R., Six, C., Lozano, J.C., Schatt, P., *et al.* (2015) Central role for ferritin in the day/night regulation of iron homeostasis in marine phytoplankton. *Proc Natl Acad Sci U S A* **112**: 14652–14657.
- Bradley, J.M., Svistunenko, D.A., Pullin, J., Hill, N., Stuart, R.K., Palenik, B., *et al.* (2019) Reaction of O₂ with a diiron protein generates a mixed-valent Fe(2+)/Fe(3+) center and peroxide. *Proc Natl Acad Sci U S A* **116**: 2058–2067.
- Bruland, K.W., Rue, E.L., and Smith, G.J. (2001) Iron and macronutrients in California coastal upwelling regimes: implications for diatoms blooms. *Limnol Oceanogr* **46**: 1661–1674.
- Caputi, L., Carradec, Q., Eveillard, D., Kirilovsky, A., Pelletier, E., Karlusich, J.J.J. *et al.* (2019) Community-level responses to iron availability in open ocean planktonic ecosystems. *Global Biogeochem Cycles* **33**: 391–419.
- Cassier-Chauvat, C., and Chauvat, F. (2014) Function and regulation of ferredoxins in the cyanobacterium, *Synechocystis* PCC6803: recent advances. *Life (Basel)* **4**: 666–680.
- Cellier, M.F., Bergevin, I., Boyer, E., and Richer, E. (2001) Polyphyletic origins of bacterial nramp transporters. *Trends Genet* **17**: 365–370.
- Coleman, M.L., and Chisholm, S.W. (2007) Code and context: *Prochlorococcus* as a model for cross-scale biology. *Trends Microbiol* **15**: 398–407.
- Dufresne, A., Ostrowski, M., Scanlan, D., Garczarek, L., Mazard, S., Palenik, B., *et al.* (2008) Unraveling the genomic mosaic of a ubiquitous genus of marine cyanobacteria. *Genome Biol* **9**: R90.
- Eddy, S.R. (2011) Accelerated profile HMM searches. *PLoS Comput Biol* **7**: e1002195.
- Eide, D.J. (2005) The zip family of zinc transporters. In *Zinc Finger Proteins*. Boston, MA: Springer, pp. 261–263.
- Eisenhut, M., Ruth, W., Haimovich, M., Bauwe, H., Kaplan, A., and Hagemann, M. (2008) The photorespiratory glycolate metabolism is essential for cyanobacteria and might have been conveyed endosymbiotically to plants. *Proc Natl Acad Sci U S A* **105**: 17199–17204.
- El-Gebali, S., Mistry, J., Bateman, A., Eddy, S.R., Luciani, A., Potter, S.C., *et al.* (2019) The Pfam protein families database in 2019. *Nucleic Acids Res* **47**: D427–D432.
- Erdner, D.L., Price, N.M., Doucette, G.J., Peleato, M.L., and Anderson, D.M. (1999) Characterization of ferredoxin and flavodoxin as markers of iron limitation in marine phytoplankton. *Mar Ecol Prog Ser* **184**: 43–53.
- Eren, A.M., Esen, O.C., Quince, C., Vineis, J.H., Morrison, H.G., Sogin, M.L., and Delmont, T.O. (2015) Anvi'o: an advanced analysis and visualization platform for 'omics data. *Peer J* **3**: e1319.
- Farrant, G.K., Dore, H., Cornejo-Castillo, F.M., Partensky, F., Ratin, M., Ostrowski, M., *et al.* (2016) Delineating ecologically significant taxonomic units from global patterns of marine picocyanobacteria. *Proc Natl Acad Sci U S A* **113**: E3365–E3374.
- Fitzsimmons, J.N., Hayes, C.T., Al-Subiai, S.N., Zhang, R., Morton, P.L., Weisend, R.E., *et al.* (2015) Daily to decadal variability of size-fractionated iron and iron-binding ligands at the Hawaii Ocean time-series station ALOHA. *Geochim Cosmochim Acta* **171**: 303–324.
- Flombaum, P., Gallegos, J.L., Gordillo, R.A., Rincón, J., Zabala, L.L., Jiao, N., *et al.* (2013) Present and future global distributions of the marine cyanobacteria *Prochlorococcus* and *Synechococcus*. *Proc Natl Acad Sci* **110**: 9824–9829.
- Galperin, M.Y., Makarova, K.S., Wolf, Y.I., and Koonin, E.V. (2015) Expanded microbial genome coverage and improved protein family annotation in the COG database. *Nucleic Acids Res* **43**: D261–D269.
- Grass, G., Franke, S., Taudte, N., Nies, D.H., Kucharski, L. M., Maguire, M.E., and Rensing, C. (2005) The metal permease ZupT from *Escherichia coli* is a transporter with a broad substrate spectrum. *J Bacteriol* **187**: 1604–1611.
- Guindon, S., Dufayard, J.F., Lefort, V., Anisimova, M., Hordijk, W., and Gascuel, O. (2010) New algorithms and methods to estimate maximum-likelihood phylogenies: assessing the performance of PhyML 3.0. *Syst Biol* **59**: 307–321.
- Hogle, S.L., Thrash, J.C., Dupont, C.L., and Barbeau, K.A. (2016) Trace metal acquisition by marine heterotrophic bacterioplankton with contrasting trophic strategies. *Appl Environ Microbiol* **82**: 1613–1624.
- Hogle, S.L., Bundy, R.M., Berube, P.M., Biller, S., Satinsky, B.M., Hackl, T., *et al.* (2018a) *Siderophore-Mediated Iron Acquisition by Marine Picocyanobacteria: Evidence for Adaptation across Ocean Basins*. Portland, OR: Ocean Sciences Meeting.
- Hogle, S.L., Dupont, C.L., Hopkinson, B.M., King, A.L., Buck, K.N., Roe, K.L., *et al.* (2018b) Pervasive iron limitation at subsurface chlorophyll maxima of the California current. *Proc Natl Acad Sci U S A* **115**: 13300–13305.
- Hopkinson, B.M., and Barbeau, K.A. (2012) Iron transporters in marine prokaryotic genomes and metagenomes. *Environ Microbiol* **14**: 114–128.
- Hopkinson, B.M., and Morel, F.M.M. (2009) The role of siderophores in iron acquisition by photosynthetic marine microorganisms. *Biometals* **22**: 659–669.
- Hutchins, D.A., and Bruland, K.W. (1998) Iron-limited diatom growth and Si: N uptake ratios in a coastal upwelling regime. *Nature* **393**: 561–564.
- Hutchins, D.A., DiTullio, G.R., Zhang, Y., and Bruland, K.W. (1995) An iron limitation mosaic in the California upwelling regime. *Limnol Oceanogr* **43**: 1037–1054.
- Jackson, S.L., Spence, J., Janssen, D.J., and Cullen, J.T. (2018) Determination of Mn, Fe, Ni, Cu, Zn, Cd and Pb in seawater using offline extraction and triple quadrupole ICP-MS/MS. *J Anal At Spectrom* **33**: 304–313.
- Kashtan, N., Roggensack, S.E., Rodrigue, S., Thompson, J. W., Biller, S.J., Coe, A., *et al.* (2014) Single-cell genomics reveals hundreds of coexisting subpopulations in wild *Prochlorococcus*. *Science* **344**: 416–420.
- Kashtan, N., Roggensack, S.E., Berta-Thompson, J.W., Grinberg, M., Stepanauskas, R., and Chisholm, S.W. (2017) Fundamental differences in diversity and genomic population structure between Atlantic and Pacific *Prochlorococcus*. *ISME J* **11**: 1997–2011.

- Kazamia, E., Sutak, R., Paz-Yepes, J., Dorrell, R.G., Vieira, F.R.J., Mach, J., *et al.* (2018) Endocytosis-mediated siderophore uptake as a strategy for Fe acquisition in diatoms. *Sci Adv* **4**: eaar4536.
- Kent, A.G., Dupont, C.L., Yooshep, S., and Martiny, A.C. (2016) Global biogeography of *Prochlorococcus* genome diversity in the surface ocean. *ISME J* **10**: 1856–1865.
- Kettler, G.C., Martiny, A.C., Huang, K., Zucker, J., Coleman, M.L., Rodrigue, S., *et al.* (2007) Patterns and implications of gene gain and loss in the evolution of *Prochlorococcus*. *PLoS Genet* **3**: e231.
- Kim, S.A., Punshon, T., Lanzirrotti, A., Li, L., Alonso, J.M., Ecker, J.R., *et al.* (2006) Localization of iron in *Arabidopsis* seed requires the vacuolar membrane transporter VIT1. *Science* **314**: 1295–1298.
- Kranzler, C., Lis, H., Shaked, Y., and Keren, N. (2011) The role of reduction in iron uptake processes in a unicellular, planktonic cyanobacterium. *Environ Microbiol* **13**: 2990–2999.
- Kranzler, C., Lis, H., Finkel, O.M., Schmetterer, G., Shaked, Y., and Keren, N. (2014) Coordinated transporter activity shapes high-affinity iron acquisition in cyanobacteria. *ISME J* **8**: 409–417.
- Ku, C., and Martin, W.F. (2016) A natural barrier to lateral gene transfer from prokaryotes to eukaryotes revealed from genomes: the 70% rule. *BMC Biol* **14**: 89.
- La Roche, J., Geider, R.J., Graziano, L.M., Murray, H., and Lewis, K. (1993) Induction of specific proteins in eukaryotic algae grown under iron-deficient, phosphorus-deficient, or nitrogen-deficient conditions. *J Phycol* **29**: 767–777.
- Langmead, B., and Salzberg, S.L. (2012) Fast gapped-read alignment with Bowtie 2. *Nat Methods* **9**: 357–359.
- Lee, M.D., Ahlgren, N.A., Kling, J.D., Walworth, N.G., Rocap, G., Saito, M.A., *et al.* (2019) Marine *Synechococcus* isolates representing globally abundant genomic lineages demonstrate a unique evolutionary path of genome reduction without a decrease in GC content. *Environ Microbiol* **21**: 1677–1686.
- Li, L., Stoeckert, C.J., Jr., and Roos, D.S. (2003) OrthoMCL: identification of ortholog groups for eukaryotic genomes. *Genome Res* **13**: 2178–2189.
- Li, Q., Huisman, J., Bibby, T.S., and Jiao, N. (2019) Biogeography of cyanobacterial *isiA* genes and their link to iron availability in the ocean. *Front Microbiol*.
- Mackey, K.R., Post, A.F., McIlvin, M.R., Cutter, G.A., John, S.G., and Saito, M.A. (2015) Divergent responses of Atlantic coastal and oceanic *Synechococcus* to iron limitation. *Proc Natl Acad Sci U S A* **112**: 9944–9949.
- Makui, H., Roig, E., Cole, S.T., Helmann, J.D., Gros, P., and Collier, M.F.M. (2002) Identification of the *Escherichia coli* K-12 Nramp orthologue (MntH) as a selective divalent metal ion transporter. *Mol Microbiol* **35**: 1065–1078.
- Malmstrom, R.R., Rodrigue, S., Huang, K.H., Kelly, L., Kern, S.E., Thompson, A., *et al.* (2013) Ecology of uncultured *Prochlorococcus* clades revealed through single-cell genomics and biogeographic analysis. *ISME J* **7**: 184–198.
- Marchetti, A., and Cassar, N. (2009) Diatom elemental and morphological changes in response to iron limitation: a brief review with potential paleoceanographic applications. *Geobiology* **7**: 419–431.
- Marchetti, A., and Maldonado, M.T. (2016) Iron. In *The Physiology of Microalgae*, B., M.A., Beardall, J., and Raven, J. A. (eds). New York: Springer, pp. 233–279.
- Marchetti, A., Parker, M.S., Moccia, L.P., Lin, E.O., Arrieta, A.L., Ribalet, F., *et al.* (2009) Ferritin is used for iron storage in bloom-forming marine pennate diatoms. *Nature* **457**: 467–470.
- Marchetti, A., Morenco, C.M., Cohen, N.R., Oleinikov, I., deLong, K., Twining, B.S., *et al.* (2017) Development of a molecular-based index for assessing iron status in bloom-forming pennate diatoms. *J Phycol* **53**: 820–832.
- Martiny, A.C., Coleman, M.L., and Chisholm, S.W. (2006) Phosphate acquisition genes in *Prochlorococcus* ecotypes: evidence for genome-wide adaptation. *Proc Natl Acad Sci U S A* **103**: 12552–12557.
- Martiny, A.C., Tai, A.P.K., Veneziano, D., Primeau, F., and Chisholm, S.W. (2009a) Taxonomic resolution, ecotypes and the biogeography of *Prochlorococcus*. *Environ Microbiol* **11**: 823–832.
- Martiny, A.C., Huang, Y., and Li, W. (2009b) Occurrence of phosphate acquisition genes in *Prochlorococcus* cells from different ocean regions. *Environ Microbiol* **11**: 1340–1347.
- Mazard, S., Ostrowski, M., Partensky, F., and Scanlan, D.J. (2012) Multi-locus sequence analysis, taxonomic resolution and biogeography of marine *Synechococcus*. *Environ Microbiol* **14**: 372–386.
- Moore, J.K., and Braucher, O. (2008) Sedimentary and mineral dust sources of dissolved iron to the world ocean. *Biogeosciences* **5**: 631–656.
- Moore, J.K., Doney, S.C., Glover, D.M., and Fung, I.Y. (2002) Iron cycling and nutrient-limitation patterns in surface waters of the world ocean. *Deep-Sea Res II* **49**: 463–507.
- Moore, L.R., Coe, A., Zinser, E.R., Saito, M.A., Sullivan, M. B., Lindell, D., *et al.* (2007) Culturing the marine cyanobacterium *Prochlorococcus*. *Limnol Oceanogr*: *Methods* **5**: 353–362.
- Morris, J.J., Lenski, R.E., and Zinser, E.R. (2012) The black queen hypothesis: evolution of dependencies through adaptive gene loss. *mBio* **3**: e00036–12.
- Ochman, H., Lawrence, J.G., and Groisman, E.A. (2000) Lateral gene transfer and the nature of bacterial innovation. *Nature* **405**: 299–304.
- Oksanen, J., Blanchet, F.G., Kindt, R., Legendre, P., O'Hara, R.B., Simpson, G.L., *et al.* (2011) Vegan: community ecology package. *R package version* **1**: 17–18.
- Olm, M.R., Brown, C.T., Brooks, B., and Banfield, J.F. (2017) dRep: a tool for fast and accurate genomic comparisons that enables improved genome recovery from metagenomes through de-replication. *ISME J* **11**: 2864–2868.
- Palenik, B., Ren, Q.H., Dupont, C.L., Myers, G.S., Heidelberg, J.F., Badger, J.H., *et al.* (2006) Genome sequence of *Synechococcus* CC9311: insights into adaptation to a coastal environment. *Proc Natl Acad Sci U S A* **103**: 13555–13559.
- Pasquier, B., and Holzer, M. (2018) The number of past and future regenerations of iron in the ocean and its intrinsic fertilization efficiency. **15**: 7177–7203.

- Pittera, J., Humily, F., Thorel, M., Grulois, D., Garczarek, L., and Six, C. (2014) Connecting thermal physiology and latitudinal niche partitioning in marine *Synechococcus*. *ISME J* **8**: 1221–1236.
- Rivers, A.R., Jakuba, R.W., and Webb, E.A. (2009) Iron stress genes in marine *Synechococcus* and the development of a flow cytometric iron stress assay. *Environ Microbiol* **11**: 382–396.
- Rocap, G., Distel, D.L., Waterbury, J.B., and Chisholm, S.W. (2002) Resolution of *Prochlorococcus* and *Synechococcus* ecotypes by using 16S-23S ribosomal DNA internal transcribed spacer sequences. *Appl Environ Microbiol* **68**: 1180–1191.
- Rusch, D.B., Martiny, A.C., Dupont, C.L., Halpern, A.L., and Venter, J.C. (2010) Characterization of *Prochlorococcus* clades from iron-depleted oceanic regions. *Proc Natl Acad Sci U S A* **107**: 16184–16189.
- Saito, M.A., Rocap, G., and Moffett, J.W. (2005) Production of cobalt binding ligands in a *Synechococcus* feature at the Costa Rica upwelling dome. *Limnol Oceanogr* **50**: 279–290.
- Scanlan, D., Ostrowski, M., Mazard, S., Dufresne, A., Garczarek, L., Hess, W., *et al.* (2009) Ecological genomics of marine Picocyanobacteria. *Microbiol Mol Biol Rev* **73**: 249–299.
- Sedwick, P.N., Church, T.M., Bowie, A.R., Marsay, C.M., Ussher, S.J., Achilles, K.M., *et al.* (2005) Iron in the Sargasso Sea (Bermuda Atlantic time-series study region) during summer: Eolian imprint, spatiotemporal variability, and ecological implications. *Global Biogeochem Cycles* **19**: GB4006.
- Shaked, Y., Kustka, A.B., and Morel, F.M.M. (2005) A general kinetic model for iron acquisition by eukaryotic phytoplankton. *Limnol Oceanogr* **50**: 872–882.
- Scholnick, S., Summerfield, T.C., Reyman, L., Sherman, L. A., and Keren, N. (2009) The mechanism of iron homeostasis in the unicellular cyanobacterium *Synechocystis* sp. PCC 6803 and its relationship to oxidative stress. *Plant Physiol* **150**: 2045–2056.
- Sohm, J.A., Ahlgren, N.A., Thomson, Z.J., Williams, C., Moffett, J.W., Saito, M.A., *et al.* (2015) Co-occurring *Synechococcus* ecotypes occupy four major oceanic regimes defined by temperature, macronutrients and iron. *ISME J* **10**: 333–345.
- Stuart, R.K., Dupont, C.L., Johnson, D.A., Paulsen, I.T., and Palenik, B. (2009) Coastal strains of marine *Synechococcus* species exhibit increased tolerance to copper shock and a distinctive transcriptional response relative to those of open-ocean strains. *Appl Environ Microbiol* **75**: 5047–5057.
- Stuart, R.K., Brahamsha, B., Busby, K., and Palenik, B. (2013) Genomic Island genes in a coastal marine *Synechococcus* strain confer enhanced tolerance to copper and oxidative stress. *ISME J* **7**: 1139–1149.
- Sunagawa, S., Coelho, L.P., Chaffron, S., Kultima, J.R., Labadie, K., Salazar, G., *et al.* (2015) Structure and function of the global ocean microbiome. *Science* **348**: 1261359–1261351.
- Sunda, W.G., and Huntsman, S.A. (1997) Interrelated influence of iron, light and cell size on marine phytoplankton growth. *Nature* **390**: 389–392.
- Tara Oceans Consortium, C. T. O. E., Participants (2015). Environmental Context of all Samples from the Tara Oceans Expedition (2009–2013), about Depth Specific Features. PANGAEA. <https://doi.org/10.1594/PANGAEA.875577>.
- Tatusova, T., DiCuccio, M., Badretdin, A., Chetvermin, V., Nawrocki, E.P., Zaslavsky, L., *et al.* (2016) NCBI prokaryotic genome annotation pipeline. *Nucleic Acids Res* **44**: 6614–6624.
- Taudte, N., and Grass, G. (2010) Point mutations change specificity and kinetics of metal uptake by ZupT from *Escherichia coli*. *Biometals* **23**: 643–656.
- Team, R. C. (2018). *R: A Language and Environment for Statistical Computing*. Vienna, Austria: R Foundation for Statistical Computing.
- Toulza, E., Tagliabue, A., Blain, S., and Piganeau, G. (2012) Analysis of the global ocean sampling (GOS) project for trends in iron uptake by surface ocean microbes. *PLoS One* **7**: e30931.
- Valasatava, Y., Rosato, A., Banci, L., and Andreini, C. (2016) MetalPredator: a web server to predict iron-sulfur cluster binding proteomes. *Bioinformatics* **32**: 2850–2852.
- Van Hove, B., Staudenmaier, H., and Braun, V. (1990) Novel two-component transmembrane transcription control: regulation of iron dicitrate transport in *Escherichia coli* K-12. *J Bacteriol* **172**: 6749–6758.
- Wuttig, K., Townsend, A.T., van der Merwe, P., Gault-Ringold, M., Holmes, T., Schallenberg, C., *et al.* (2019) Critical evaluation of a seaFAST system for the analysis of trace metals in marine samples. *Talanta* **197**: 653–668.
- Xia, X., Cheung, S., Endo, H., Suzuki, K., and Liu, H. (2019) Latitudinal and vertical variation of *Synechococcus* assemblage composition along 170 degrees W transect from the South Pacific to the Arctic Ocean. *Microb Ecol* **77**: 333–342.
- Zwirgmaier, K., Jardillier, L., Ostrowski, M., Mazard, S., Garczarek, L., Vaulot, D., *et al.* (2008) Global phylogeography of marine *Synechococcus* and *Prochlorococcus* reveals a distinct partitioning of lineages among oceanic biomes. *Environ Microbiol* **10**: 147–161.

Supporting Information

Additional Supporting Information may be found in the online version of this article at the publisher's web-site:

Appendix S1: Supplementary Materials

Appendix S2: Supplementary Materials